Time-Resolved Fluorescence and Absorption Spectroscopy of Photosystem I†

Gary Hastings, Frank A. M. Kleinherenbrink, Su Lin, and Robert E. Blankenship*

Department of Chemistry and Biochemistry and the Center for the Study of Early Events in Photosynthesis, Arizona State University, Tempe, Arizona 85287-1604

Received November 5, 1993; Revised Manuscript Received January 24, 1994®

ABSTRACT: Picosecond fluorescence and femtosecond transient absorption spectroscopy have been used to investigate the primary energy transfer and trapping processes in a photosystem II deletion mutant from the cyanobacterium *Synechocystis* sp. PCC 6803, which contains active photosystem I reaction centers with ~100 chlorophylls per P700. In all experiments, low levels of excitation were used which avoid annihilation processes. Following 590-nm excitation, at room temperature, spectral equilibration is observed in both fluorescence and absorption measurements and is characterized by a time constant of 4–6 ps. The shape of the spectra associated with the equilibration process indicates that long wavelength pigments (pigments with absorption maxima at longer wavelength than that of the primary electron donor, P700) are present and functional at physiological temperatures in this preparation. The overall decay of excitations in the antenna is characterized by a time constant of 24–28 ps, in both fluorescence and absorption measurements. The 24–28-ps process results in the appearance of absorption changes associated with only $P700^+$ formation. Absorption changes associated with the reduction of the primary electron acceptor were not resolved under the experimental conditions used here.

Electron and energy transfer reactions in photosynthetic systems has been a subject of considerable interest for many decades [see van Grondelle (1985), Holzwarth (1989), and Martin and Vos (1992) for reviews]. The advent of pico/femtosecond laser systems has resulted in the development of techniques which allow the direct observation of these electron and energy transfer reactions. Time-resolved fluorescence and absorption experiments, with (sub)picosecond time resolution, are two techniques that have been widely used to investigate the initial electron and energy transfer processes in photosystem I (PS I).[1] These experiments were performed using PS I particles isolated from a variety of species with widely varying antenna sizes [see Sétif (1992) and Holzwarth (1991) for reviews].

The structure and organization of the PS I core antenna complex is a subject of intense research (Werst et al., 1992; Jia et al., 1992; Laible & Owens, 1993). The Q_y absorption peak in most PS I preparations at room temperature is asymmetric and has a FWHM >25 nm, indicating a relatively large distribution of spectral forms in the PS I core antenna. This large distribution of spectral forms is present even in PS I particles that contain only 10 chlorophylls/P700 (Ikegami & Itoh, 1988), which indicates that spectral heterogeneity is present even in the few chlorins of the core antenna that are presumably in close proximity to the primary electron donor, P700.

A related question concerning spectrally heterogeneous antenna systems is the role of long wavelength chlorophylls (Chls) that absorb at longer wavelengths than the primary electron donor (we shall refer to these pigments as "red pigments" below). The lack of observation of fluorescence emission from the red pigments at room temperature has led some authors to suggest that these red pigments may be a low temperature induced artifact (Holzwarth, 1991; Satoh & Butler, 1978; Butler, 1978). It has been estimated that, in the PS I particles that were used in the present study, there are ~8–11 red pigments/P700. At 295 K these red pigments absorb maximally at 703 nm (Woolf et al., 1994).

The functional role of the red pigments is still unclear. It has been proposed that long wavelength pigments serve to focus excitations in the vicinity of the traps (van Grondelle & Sundström, 1988). This proposal has been questioned because having red pigments situated near the traps may lead to a decreased trapping efficiency, as energy has to be transferred "uphill" from a red pigment to P700 (Beauregard et al., 1991; Fischer & Hoff, 1992; Trissl, 1993).

Although it would appear that having red pigments near the reaction center may introduce some inefficiency to the trapping process, recent computer simulations (Jia et al., 1992) indicate that one or two red pigments in the vicinity of the trap, with the remainder of the spectral forms in the core antenna distributed randomly, best describes the observed temperature dependence of the fluorescence decays in PS I particles from *Chlamydomonas reinhardtii* (Werst et al., 1992). Furthermore, Trissl (1993) has shown that long wavelength pigments need not constitute a major kinetic limitation at room temperature. Trissl (1993) indicated that the real advantage of red pigments may not be purely related to kinetic efficiency. The development of red pigments may result in a biological advantage by increasing the effective absorption cross section to spectrally filtered light.

There is some disagreement in the literature concerning the details of excitation migration in the PS I core antenna. PS I particles from spinach display a polarization pattern that suggests a pebble mosaic model may provide an appropriate description of the core antenna of these particles (Causgrove et al., 1988; Struve et al., 1990), with equilibration within individual polypigment units taking place in a few picoseconds and energy transfer between different units taking

† This work was supported by NSF Grant DMB-9106685.

* Author to whom correspondence should be addressed.

® Abstract published in *Advance ACS Abstracts,* March 1, 1994.

[1] Abbreviations: (B)Chl *a*, (bacterio)chlorophyll *a*; FWHM, full width at half-maximum; LHC I, light harvesting complex I; PS I, photosystem I; DAS, decay associated spectrum; P700, primary electron donor in PS I; A_0, primary electron acceptor in photosystem I; A_1, secondary electron acceptor in photosystem I; TX-100, Triton X-100; PMS, phenazine methosulfate.

0006-2960/94/0433-3185$04.50/0

between 5 and 15 ps. In contrast, Du et al. (1992) observed a very different polarization pattern in PS I particles from *C. reinhardtii*, which indicates that such a model may not be appropriate for these particles.

Turconi et al. (1993) observed a 12-ps time constant (and suggested there may be faster, unresolved lifetimes), which they assigned to equilibration between spectrally different pools of chlorins [it should be noted that Turconi et al. (1993) analyze their data in terms of spectrally different pools which does not necessarily mean spatially distinct pools]. In contrast, Klug et al. (1989) observed that, in PS I particles from spinach, the absorbance difference spectrum was red-shifted relative to the ground state absorption in less than 3 ps, indicating that spectral equilibration among the different chlorophylls must have occurred within this time.

Trissl et al. (1993) found that the trapping kinetics in PS I stacked pea thylakoids were independent of excitation wavelength, leading to the conclusion that the excitation energy equilibrates rapidly among all the spectral forms prior to trapping. Trissl et al. (1993) further concluded that the kinetics in PS I are trap limited, and although there are a number of long wavelength chlorins, their location relative to P700 is not of great importance at room temperature. This conclusion, however, can only be drawn if it is clear that the final energy transfer step to the trap is not limited by, for example, the distance between donor and acceptor.

Trapping in PS I has been recently reviewed (Sétif, 1992). Observed time constants that characterize the overall decay of excitations in the PS I antenna depend on the type of particle used, and lifetimes between 20 and 80 ps have been reported (Owens et al., 1987, 1988; Wittmershaus et al., 1987; Hodges & Moya, 1988; Klug et al., 1989; Trissl et al., 1993; Turconi et al., 1993; Holzwarth et al., 1993). In the past there have been some discrepancies between transient absorption and fluorescence measurements, performed using comparable particles [see Holzwarth (1991) for a review]. Recently, however, Holzwarth et al. (1993) have used both transient absorption and fluorescence to investigate the antenna kinetics in PS I particles from *Synechococcus* sp. Using both techniques, a lifetime of 35 ps is observed and assigned to the decay of excitations in the antenna.

The apparent discrepancies concerning both the mechanisms and time constants that characterize spectral equilibration and trapping in PS I are far from being resolved. The kinetics in PS I particles may, to some extent, depend on the harsh detergent treatments used in the isolation and purification of the particles (Nechushtai et al., 1986; Wittmershaus et al., 1987; Owens et al., 1988; Turconi et al., 1993). To avoid any possible ambiguity, we have used PS I cyanobacterial membrane fragments that have not been subjected to harsh detergent treatment and therefore represent a relatively intact system.

This paper describes the use of both time-resolved fluorescence and absorption spectroscopies to investigate the energy transfer and charge separation processes in a PS II deletion mutant from the cyanobacterium *Synechocystis* sp. PCC 6803, which contains only the PS I reaction center, with ~100 Chl *a* per P700 (Vermaas et al., 1987, 1988). The cyanobacterial preparations used in this study lack the peripheral antenna complex of higher plants, termed light harvesting complex I (LHC I). It is generally believed, however, that the cyanobacterial PS I core preparations are closely equivalent to the higher plant PS I core complexes that have been stripped of LHC I (Cantrell & Bryant, 1987).

We demonstrate that, in the PS I preparations used here, red pigments clearly do exist at physiological temperatures. We show that the initially excited distribution of chlorins equilibrates rapidly among all the spectral forms and that trapping proceeds from this spectrally equilibrated distribution of chlorins. From the observed kinetics we estimate an upper limit of 1.6 ps for the intrinsic time constant of radical pair formation. We also show that the overall kinetics are similar in different PS I particles but that the structure/organization of the PS I core antenna is species dependent.

MATERIALS AND METHODS

Thylakoid Preparation. The mutant psbDI/C/DII from *Synechocystis* sp. PCC 6803, which lacks PS II, was described previously (Vermaas et al., 1987, 1988). This mutant contains no major PS II proteins (Vermaas et al., 1988). Cells were grown in two 12-L glass containers at 30 °C in BG 11 medium plus 5 mM glucose. Illumination was provided by five 20-W fluorescent tubes placed ~50 cm from the containers. The medium was aerated continuously and cells were harvested after 3–4 days. Cells were harvested using a continuous flow centrifuge (approximately 1.8 g of cells were obtained per liter) and resuspended in buffer containing 50 mM Hepes, pH 7, 5 mM $MgCl_2$, 25 mM $CaCl_2$, 10% glycerol, and 0.5% DMSO. The cells were then passed three times through a French pressure cell at 20 000 psi. All preparation procedures after and including cell breakage were carried out at 4 °C. Unbroken cells and large cell debris were removed by centrifugation at 4000 rpm for 4 min in a Sorvall SS-34 rotor. The resultant supernatant was recentrifuged at 16 000 rpm for 20 min to pellet the membrane fragments. The pellet contains the membrane fragments and the supernatant contains most of the phycobilisomes. Remaining phycobilisomes were removed as described by Wittmershaus et al. (1992). Membrane fragments were stored at −70 °C until further use. Chlorophyll concentrations were determined spectrophotometrically in 80% acetone. An extinction coefficient of 82 for 1 mg/mL chlorophyll at 663 nm was used. For transient absorption experiments the chlorophyll concentration was estimated to be 55 ± 10 μg/mL.

Femtosecond Transient Absorption Measurements. All experiments described here were performed at room temperature. Samples were suspended in buffer containing 20 mM Tris-HCl, pH 8.0, approximately 20 mM ascorbate, and 10 μM phenazine methosulfate (PMS).

The sample was loaded in a spinning cell with an optical pathlength of 2.5 mm and a diameter of 18 cm. The absorbance of the sample in the cell was 1.2–1.4 at the peak of the Q_y absorption band (680 nm).

The laser system has been described (Taguchi et al., 1992; Lin et al., 1994). Briefly, 1064-nm pulses from a mode-locked Nd-YAG laser are compressed, frequency doubled, and then used to pump a dye laser. The 590-nm output pulses from the dye laser are further compressed to ~150 fs (FWHM) and then amplified to ~1 mJ/pulse using intense 532-nm, 100-ps pulses from a regenerative amplifier operating at 540 Hz, which is seeded by splitting of a small portion of the 1064-nm pulses from the mode-locked Nd-YAG laser. The amplified pulses are split, and one portion is used to generate a spectral continuum in a 1-cm flowing water cell, while the other portion is used to form the pump beam. The spectral continuum is further split into two identical parts and used to form the probe and reference beams. The pump beam was attenuated using neutral density filters and focused to excite a 3 mm^2 area of the sample. The cylindrical sample cell was rotated at 2 Hz to ensure that the pumped volume was replaced between each laser flash.

The variable time delay of the probe and reference beams relative to the pump beam was provided by a computer-controlled translation stage. The probe and the reference signals were focused onto two separate optical fibers coupled to a monochromator (Acton Research Corporation model Spectra Pro 275). The spectra were acquired over a 140-nm interval on a dual array multichannel detector (Princeton Instruments models DPAA-1024 and ST121) with 0.14 nm per channel. Prior to global analysis the data were averaged over 15 channels, resulting in a 2-nm interval between data points in each spectrum. Spectra at each time delay were obtained by averaging 1080 laser shots.

All transient absorption experiments described here were performed using 590-nm excitation, with the pump and probe beams set at the magic angle. Data were collected between 0 and 90 ps and 0–12 ps, in the 640–780-nm spectral region. The 590-nm excitation pulses were attenuated so that ~0.25 photons were absorbed per reaction center (see discussion). At this level of excitation, effects due to singlet annihilation can be excluded. This conclusion was confirmed by the fact that the same kinetics were observed when the excitation intensity was increased by a factor of 3.

Transient absorption data were collected as a function of both time delay and wavelength. The data were analyzed globally using locally written software, where the whole ΔOD–wavelength–time surface could be analyzed simultaneously. Lifetimes were calculated using a least-squares fitting algorithm assuming multiexponential kinetics. Checks were made for consistency between data collected on different time scales. The quality of the fits was assessed using a reduced χ^2 criterion and plots of weighted residuals.

Prior to each set of femtosecond transient absorption measurements, the kinetics of $P700^+$ re-reduction were monitored at 700 nm on a millisecond flash spectrometer. The concentrations of PMS and ascorbate were adjusted such that the ground state had completely recovered in less than 80 ms. Therefore, in femtosecond transient absorption experiments, we expect insignificant buildup of reaction centers with P700 oxidized. Using the same sample conditions as described for femtosecond transient absorption experiments above, the optical density change at 700 nm due to P700 oxidation, under saturating light conditions, was also monitored on the millisecond spectrometer and was $(10 \pm 2) \times 10^{-3}$. Excitation levels were estimated on the basis of the above observation and the transient bleaches (see Figure 1).

Results obtained from global analysis are presented as decay associated spectra (DAS). A decay associated spectrum is the amplitude spectrum associated with a specific kinetic component: Data are analyzed assuming a sum of exponential components, and the decay associated spectra are the spectra of the preexponential factors (Causgrove et al., 1990). From this definition it can be seen that a positive amplitude in a DAS corresponds to a negative change in the absorption difference spectrum as a function of time. Conversely, a negative amplitude in a DAS corresponds to a positive change in the absorption difference spectrum as a function of time.

Time-Resolved Fluorescence Measurements. The single photon counting system has been described previously (Causgrove et al., 1990). All experiments were performed using 590-nm excitation at 3.8-MHz repetition rate. Taking into account the high laser repetition rate and the fact that we did not flow the sample, we expect the PS I particles to be in the closed state (P700 oxidized). Therefore, the single photon counting measurements only probe changes in fluorescence associated with the antenna. We show below, and in the following paper in this issue, that the kinetics in the PS I core antenna are the same in both open (P700 neutral) and closed (P700 oxidized) traps, which confirms the results of a number of previous studies (Owens et al., 1988; Klug et al., 1989; Turconi et al., 1993).

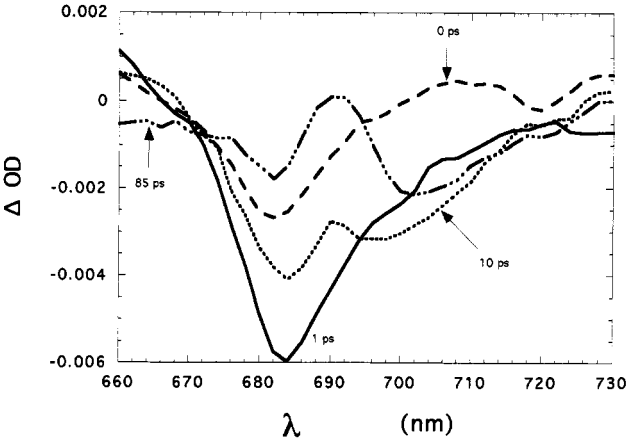

FIGURE 1: Difference spectra obtained at four different time delays, following low intensity, 590-nm excitation of PS I particles from *Synechocystis* sp. PCC 6803, at room temperature. The 0-, 1-, and 10-ps spectra were taken from data collected on a 12-ps time scale. The 85-ps spectrum was obtained from data collected on a 90-ps time scale. The excitation intensities used in the two sets of experiments were the same. The 1- and 10-ps spectra obtained from data collected on a 90-ps time scale are essentially the same as shown here.

Data were collected in 20-nm intervals between 660 and 740 nm, at room temperature. Data were collected on a 4-ns time scale, which correspond to 2 ps per channel. The fluorescence decays, obtained at six emission wavelengths, were globally analyzed with deconvolution of the measured instrument response function (~40 ps FWHM). Comparison of the results obtained from global analysis of the transient absorption and fluorescence data (Figures 2 and 4) indicate that lifetimes of a few picoseconds can be well resolved in the single photon counting experiments.

RESULTS

Transient Absorption Measurements. Transient absorption data were collected simultaneously as a function of both time and wavelength. Data were collected between 640 and 780 nm, on both a 12- and 90-ps time scale. Figure 1 shows the spectra obtained at a variety of time delays following low intensity, 590-nm excitation. The 1-ps difference spectrum displays a bleaching which peaks at 684 nm. Between 1 and 10 ps this initial bleaching partially recovers on the short wavelength side, and a rise or grow-in of a bleaching is observed on the longer wavelength side. Between 10 and 85 ps the bleaching in the 670–715-nm region recovers further and results in a spectrum that does not decay further on the time scales considered here.

Data collected at 70 wavelengths between 640 and 780 nm, and at 100 time delays (four are shown in Figure 1), were analyzed globally. Global analysis of data on each time scale was performed separately, and checks were made for consistency in the results of the separate analyses. Table 1 summarizes the lifetimes obtained from the different analyses. Data obtained on a 90-ps time scale could be well described by two exponential components, with lifetimes of 5 and 28 ps, and a nondecaying component. The lifetime and amplitude of the faster component is not well resolved in data collected on a 90-ps time scale. Data obtained on a 12-ps time scale could be well described by three exponential components with

Table 1: Lifetimes Obtained from Global Analysis of Transient Absorption and Fluorescence Data

	transient absorption		
	12-ps time scale	90-ps time scale	fluorescence
lifetimes	560 fs		
	4 ps	5 ps	6 ps
	32 ps[a]	28 ps	24 ps
		4.5 ns[a]	238 ps
			825 ps
			3.5 ns

[a] Nondecaying on the time scale considered.

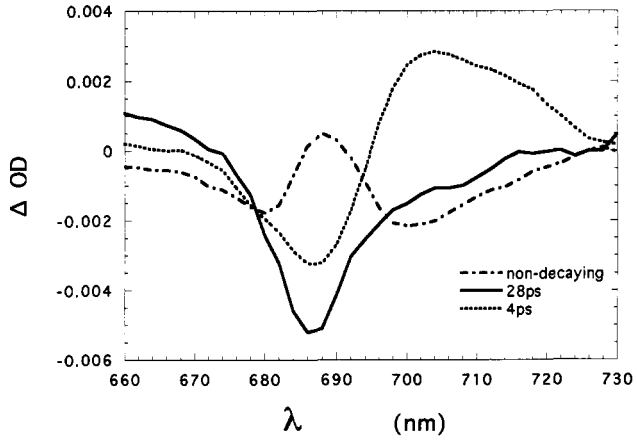

FIGURE 2: Decay associated spectra of the 4-ps (dotted line), 28-ps (solid line), and nondecaying (dot-dashed line) components obtained from global analysis of transient absorption data collected using PS I particles from *Synechocystis* sp. PCC 6803. Data were collected on two different time scales, at room temperature. The 4-ps component is obtained from global analysis of data collected on a 12-ps time scale. The 28-ps and nondecaying components were obtained from analysis of data collected on a 90-ps time scale. The data obtained on both time scales have not been normalized because the excitation intensities used in both sets of experiments were the same.

lifetimes of 560 fs, 4 ps, and 32 ps. The spectrum of the 32-ps component is essentially nondecaying on a 12-ps time scale and is similar to the sum of the 28-ps and nondecaying components, obtained from analyses of data on a 90-ps time scale. The 560-fs time constant is needed to adequately describe the data (Figure 3); however, the lifetime is near our time resolution limit, and the spectrum of this component cannot be adequately separated from the instrumental rise without deconvolution. Because the 560-fs component cannot be clearly resolved, we shall not consider it here. However, we note that the spectrum of the 4-ps component, obtained from analysis of data collected on a 12-ps time scale, depends to some extent on whether the faster component is included in the analysis.

Excluding the 560-fs component, it appears that two exponential components, with lifetimes of 4 and 28 ps, and a nondecaying component are sufficient to adequately describe the data obtained on both time scales between 640 and 780 nm. The nondecaying component decays in the millisecond time range (see below and following paper) and is essentially constant on the time scales considered here. The decay associated spectra (DAS) of the 4 ps, 28 ps, and nondecaying components are shown in Figure 2.

The 4-ps spectrum in Figure 2 has a negative peak at 686 nm but is positive on the longer wavelength side. The negative peak at 686 nm is due to the decay of an initial bleaching while the positive peak is due to the rise or grow-in of a bleaching (see Figures 1 and 3). The shape of this spectrum

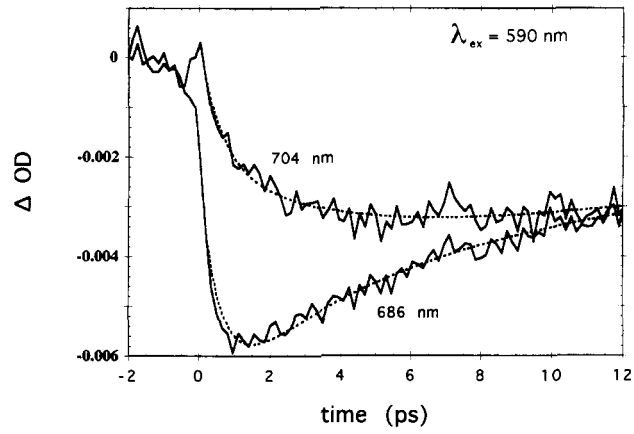

FIGURE 3: Kinetics of the absorption changes observed at 686 and 704 nm, between 0 and 12 ps, following 590-nm excitation of PS I particles from *Synechocystis* sp. PCC 6803, at room temperature. The fitted functions, obtained from global analysis, are also shown (dotted lines). These fitted functions are the sum of three exponential components with lifetimes of 0.56, 4, and 32 ps.

is characteristic of an energy transfer process, from pigments that absorb maximally in the 680-nm spectral region to pigments that absorb predominately above 700 nm.

The 28-ps spectrum in Figure 2 displays a negative peak at 686 nm and has considerable amplitude on the longer wavelength side, indicating that long wavelength chlorins contribute to the process(es) which give rise to the 28-ps component. The negative amplitude of the 28-ps spectrum in the 680–720-nm spectral region corresponds to the recovery of a bleaching in this wavelength region (see Figures 1 and 3).

Figure 3 compares the kinetics observed at 686 and 704 nm. A clear rise time or grow-in of a bleaching is observed at 704 nm during the first few picoseconds. Essentially the opposite is observed at 686 nm. Figure 3 demonstrates that an energy transfer process, characterized by a time constant of 4 ps, is clearly well resolved in our data. Figure 3 also shows the fitted functions obtained from the three-component analysis of data collected on a 12-ps time scale. A faster 560-fs lifetime has to be included to adequately describe the early time course of the absorption changes (see above).

Single Photon Counting Measurements. In order to further investigate the kinetics in PS I particles from *Synechocystis* sp. PCC 6803, and to complement the transient absorption studies, we have also performed time-resolved fluorescence measurements with picosecond time resolution. Experiments were performed with the PS I reaction centers in the closed state (P700 is oxidized by the excitation beam), although this should not greatly affect the antenna kinetics (Owens et al., 1988; Turconi et al., 1993; see also Materials and Methods).

A minimum of five exponential components are required to adequately fit the fluorescence data, collected at five wavelengths between 660 and 740 nm, on a 4-ns time scale (as judged by the reduced χ^2 parameter and plots of weighted residuals). The lifetimes of the exponential components are 6 ps, 24 ps, 238 ps, 825 ps, and 3.5 ns. The DAS of these exponential components are shown in Figure 4. Figure 4 demonstrates that the fluorescence decays are dominated by the two fastest components, which account for more than 98% of the total decay amplitude at all wavelengths except 660 nm. The 24-ps component peaks around 686 nm and is broader on the long wavelength side. The 6-ps component has a positive peak near 680 nm and a negative peak near 720 nm. The shape of the 6-ps spectrum clearly indicates that it is due to an energy transfer process in which energy is transferred from

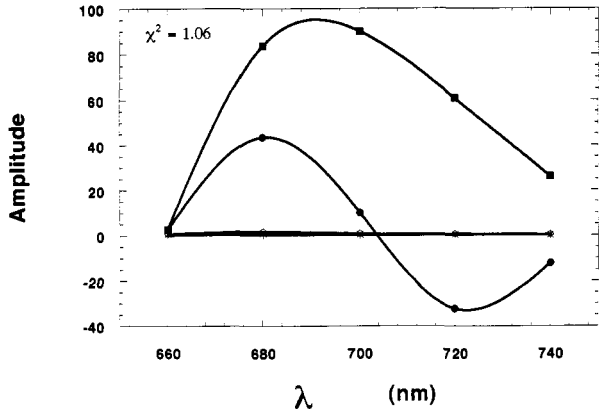

FIGURE 4: Decay associated spectra with lifetimes of 6 ps (●), 24 ps (■), 238 ps (◇), 825 ps (×), and 3.5 ns (+), obtained from global analysis of time-resolved fluorescence data. Fluorescence data were collected following 590-nm excitation of PS I particles from *Synechocystis* sp. PCC 6803, at room temperature. Data were collected between 0 and 4 ns (which corresponds to 2 ps per channel). The high laser repetition rate results in closure of the traps (P700 oxidized).

chlorins that emit below 700 nm to chlorins that emit above 700 nm. The lifetimes obtained from the fluorescence data for the two fastest components are identical (within error) to the lifetimes obtained from global analysis of the transient absorption data.

DISCUSSION

Spectral Equilibration in the PS I Core Antenna. The shape of the 4-ps DAS in Figure 2 and the 6-ps DAS in Figure 4 are characteristic of an energy transfer process. The DAS clearly indicate that long wavelength pigments are present and functional at room temperature, in the PS I particles used in this study.

The energy transfer process is a result of a relaxation of the initially excited distribution of pigments to the Boltzmann distribution. We therefore assign the 4–6-ps lifetime to equilibration of excitation energy between the various spectral forms in the PS I core antenna. Equilibration of excitation energy in the PS I core antenna depends on the spatial organization of the different spectral forms. Since we have no knowledge of this spatial organization, we shall use the term spectral equilibration to describe the 4–6-ps equilibration process that is observed following excitation. The interpretation of the 4-ps (6-ps) DAS in both transient absorption and fluorescence is the same, and the lifetimes obtained are within error identical. The absorption measurements have superior time resolution, and we shall therefore refer to the lifetime of this energy transfer process as 4 ps.

Recently, Turconi et al. (1993) have observed a similar energy transfer process, characterized by a 12-ps time constant, in PS I-100 particles from *Synechococcus* sp. This was the first clear indication from time-resolved fluorescence measurements that pigments with absorption maxima at longer wavelengths than that of the primary electron donor do exist at physiological temperatures in PS I. Holzwarth et al. (1993) have recently performed transient absorption measurements on the same particles as used by Turconi et al. (1993). These authors observe a DAS that is characteristic of an energy transfer process, with lifetime of 8 ps. They suggest that the difference in lifetime between fluorescence and absorption measurements is due to unresolved energy transfer components, with lifetimes less than 3 ps, that affect their absorption measurements but not their fluorescence measurements. We obtain an overall lifetime for energy transfer to long wavelength chlorins of 4 ps. We do not find any evidence for a component with lifetime of ~10 ps, although we could almost certainly resolve such a lifetime if it were present with appreciable amplitude. The apparent discrepancy in lifetimes is unresolved at present; however, there are a number of possible explanations.

Our particles are membrane fragments that have not been subjected to harsh detergent treatment. Although Holzwarth et al. (1993) also appear to have a homogeneous, well characterized PS I preparation, which was obtained by treating the membrane fragments with TX-100, it may be that the kinetics in PS I particles depend to some extent on the detergent treatment (Nechushtai et al., 1986; Wittmershaus et al., 1987; Owens et al., 1988). Because we have worked directly on the membrane fragments, we can eliminate any possibility of detergent-induced artifactual kinetics.

Beauregard et al. (1991) have shown that the overall lifetime and shape of a DAS associated with spectral equilibration (in a random model with long wavelength pigments near the primary electron donor) depends strongly on the degree of spectral heterogeneity and the excitation wavelength. Holzwarth et al. (1993) and Turconi et al. (1993) used 678-nm excitation, whereas we have used 590-nm excitation in both fluorescence and absorption experiments. The apparent differences in lifetimes obtained may therefore also be due to differences in excitation wavelength. We will show below that the core antenna structure/organization is clearly different in PS I particles isolated from different species. This may also provide an explanation for the apparent discrepancy in time constants for this energy transfer process.

Overall Decay of Excitations in the PS I Core Antenna. The spectrum of the 28-ps component in Figure 2 displays a negative peak at 686 nm and is broader or asymmetric on the long wavelength side. The negative amplitude of the 28-ps spectrum (Figure 2) in the 675–730-nm spectral region results from the decay of an initial bleaching (see Figures 1 and 3). The simplest interpretation of the 28-ps spectrum is that it is a result of overall decay of the excitations in the antenna, due to trapping. Absorption changes associated with both $P700^+$ formation and the decay of excitations in the antenna contribute to the 28-ps spectrum. The negative amplitude of the 28-ps spectrum in the 700-nm region is therefore less than would be expected for only the decay of excitations in the antenna (the 10-ps spectrum in Figure 1 roughly shows the difference spectrum associated with the equilibrated distribution of excitations in the antenna). The above considerations indicate that red pigments contribute significantly to the 28-ps process(es) and, therefore, the processes responsible for the 28-ps component proceed from a thermally relaxed or spectrally equilibrated state. Identical conclusions can be drawn for the 24-ps emission spectrum in Figure 4. The shape of the 24-ps fluorescence spectrum is consistent with the decay of excited states of pigments that emit in the 680-nm spectral region and above 700 nm. The overall shape of the 24-ps spectrum is similar to the shape of the steady-state fluorescence spectrum at 296 K (Wittmershaus et al., 1992). The overall similarity in shape provides further support for the conclusion that the 24-ps component is a result of overall decay of excitations in the spectrally equilibrated antenna. The lifetimes assigned to this process, from both fluorescence and absorption data, are again identical within error. A lifetime of 28 ps, for overall decay of excitations in the antenna, is in good agreement with other studies (Hodges & Moya, 1988;

Owens et al., 1988; Turconi et al., 1993; Holzwarth et al., 1993).

Pigment Content. The shape of the 4-ps spectrum in Figure 2 provides strong evidence that long wavelength pigments exist at physiological temperatures in PS I core particles from *Synechocystis* sp. PCC 6803, in agreement with recent steady state, polarized fluorescence studies performed using the same particles as were used here (Woolf et al., 1994). The work of Turconi et al. (1993), as well as the work presented here, indicates that long wavelength pigments clearly do exist at physiological temperatures, in two different strains of cyanobacteria. We have recently performed experiments using PS I-60 and PS I-100 particles isolated from spinach and also found clear evidence for the existence of long wavelength pigments (G. Hastings, S. Hoshina, F. A. M. Kleinherenbrink, and R. E. Blankenship, unpublished data). It therefore appears that long wavelength chlorins may be a universal characteristic of the PS I core antenna.

The spectra in Figure 1 include contributions from both stimulated emission and photobleaching. In the following, we shall assume that stimulated emission results in a ~3–5-nm (i.e., 4 ± 1 nm) red-shift of observed bleachings, relative to the steady-state absorption peaks of the pigments (Klug et al., 1987; Holzwarth et al., 1993). The 1-ps spectrum consists predominately of contributions from pigments that absorb near 680 nm. The 590-nm excitation is probably absorbed nearly equally by all the pigments in the antenna (via excitation of the higher vibronic or Q_x absorption bands (Hoff & Amesz, 1991, and references therein) of the pigments). However, it is difficult to assess what contribution longer wavelength chlorins make to the 1-ps difference spectrum, because excited state absorption from the excited, 680-nm pigments masks bleachings due to excitation of the red pigments.

The 10-ps spectrum in Figure 1 essentially represents the difference spectrum due to the equilibrated distribution of excitations prior to trapping. The spectrum displays bleachings that peak at 684 and 697 nm, the longer wavelength bleaching extending to ~720 nm. Therefore, the 10-ps spectrum suggests that, in addition to the large group of chlorins that absorb near 680 nm, there appears to be a group of chlorins that absorb near 693 nm (assuming that the absorption peak is 4-nm blue-shifted relative to the observed bleaching because of stimulated emission). Furthermore, it is clear from recent polarized fluorescence studies that there are a group of chlorins that absorb at 703 nm (Woolf et al., 1994). Therefore, in the PS I particles used here, there appear to be at least three distinct groups of pigments that absorb near 680, 693, and 703 nm. It is not possible to calculate from the difference spectra in Figure 1 the relative stoichiometry of each group of pigments without performing a spectral decomposition and assuming some model to describe the equilibration process among the different pigment groups. Such a model, which would include forward and reverse rate constants describing equilibration between more than two groups of chlorins, is difficult to solve without the use of a number of simplifying assumptions. Models which include equilibration between two pools, followed by charge separation, have been described by Turconi et al. (1993). These authors recognize that their modeling may be oversimplified; however, the solutions to more complicated models have not yet been presented. In a very approximate calculation, Holzwarth et al. (1993) estimated that, in PS I particles from *Synechococcus* sp., there are 81, 15, and 4 pigments that absorb maximally at 680, 695, and 710 nm, respectively. We are unable to calculate the number of pigments that absorb at wavelengths below 700 nm. However, the considerations outlined above suggest that there are differences in both the number and spectral nature of the longest wavelength pigments in the different cyanobacterial PS I core antennae. Whether the above differences in the number of red pigments represent differences in the preparations or result from the different methods used to detect them is not yet resolved.

The 28-ps spectrum in Figure 2, which is a result of overall decay of excitations in the spectrally equilibrated antenna, peaks at 686 nm. The spectra for the corresponding process in PS I particles from *Synechococcus* sp. peaks near 715 nm [see Figure 5 of Holzwarth et al. (1993)]. This difference cannot be related to differences in the amounts of uncoupled chlorophyll in the different particles (Holzwarth et al., 1993). The fact that the same process is characterized by very different spectra in the different PS I particles is a clear indication that the antenna structure/organization is different in the different cyanobacterial PS I preparations and, as suggested above, may explain the differences in time constants characterizing the equilibration processes in the different cyanobacterial PS I particles.

Although the kinetic processes are similar in the different cyanobacterial PS I preparations, there appear to be differences in the spectral composition of the different cyanobacterial PS I core antennae (see above). It is not clear if differences in spectral composition alone can account for the differences in the DAS that represent the decay of antenna excitations in the different particles. It is unclear to what extent the spatial organization of the pigments in the different preparations also contributes to the differences in the DAS associated with trapping.

Radical Pair Formation. The nondecaying difference spectrum shown in Figure 2 represents a state that does not decay on the time scales considered here. The spectrum shows bleachings at 680 and 700 nm and a positive peak near 688 nm. This nondecaying spectrum is similar in shape to published ($P700^+ - P700$) difference spectra (Schaffernicht & Junge 1981, 1982; Hiyama & Ke, 1972; see also Figure 4 in the following paper). The nondecaying spectrum in Figure 2 is due only to $P700^+$ formation and contains no contribution from absorption changes associated with the primary electron acceptor. This interpretation follows from the detailed discussion of data obtained using high intensity excitation that is presented in the following paper. Since the 28-ps process results in a difference spectrum that is due only to P700 oxidation, it follows that either the primary electron acceptor does not absorb in this spectral region or the reduced acceptor decays faster than it forms. We show in the following paper that the latter hypothesis is appropriate and may explain why absorption changes associated with the primary electron acceptor have never been observed in a transient absorption experiment under normal conditions (P700 neutral) when low excitation intensities are used (Klug et al., 1989; Holzwarth et al., 1993; see also following paper in this issue).

From transient absorption experiments on a millisecond time scale, utilizing saturating light excitation and the same sample conditions as for the femtosecond transient absorption experiments, we have determined that the optical density change at 700 nm, due to 100% P700 oxidation is $(10 \pm 2) \times 10^{-3}$. The nondecaying spectrum in Figure 2 shows that the bleaching at 700 nm is $\sim 2.2 \times 10^{-3}$. This indicates that our excitation intensities are such that $P700^+$ is formed in (22.5 ± 4.5)% of the PS I reaction centers in the illuminated volume. This result is also consistent with the magnitude of the initial bleaching we observe following excitation, relative to the

ground state absorption [assuming stimulated emission accounts for 50% of the initial bleaching and that there are ~100 Chls per reaction center (see below)].

Using a difference extinction coefficient of 64 mM^{-1} cm^{-1} (Hiyama & Ke, 1972) for P700 oxidation at 700 nm, in addition to the measured Chl concentration of ~55 μg/mL, we estimate that the particles used in this study contain 98 ± 20 Chls per P700. This value is in good agreement with the results of a number of other studies of cyanobacterial PS I preparations (Hefti et al., 1992; Boekema, 1987).

Trapping-Limited versus Diffusion-Limited Kinetics. The kinetics of the trapping process in PS I reaction center complexes have been widely discussed (Hodges & Moya, 1988; Owens et al., 1987, 1988; Holzwarth et al., 1993; Trissl, 1993). Two extreme cases are usually considered: (1) The overall trapping rate is limited by the time it takes the excitations to migrate to the reaction center (termed the diffusion-limited case). (2) The trapping rate is limited by the intrinsic rate of the charge separation process. This is usually referred to as the trapping-limited case. In this case the excitation has a finite probability of escaping back to the antenna from the trap (Pearlstein, 1982).

In our measurements on PS I particles from *Synechocystis* sp. PCC 6803, a fast spectral equilibration is observed (which indicates ultrafast energy transfer between neighboring pigments), followed by a much slower decay of excitations in the antenna due to charge separation. These observations alone indicate that a diffusion-limited kinetic model cannot adequately describe the trapping process in the PS I particles used here.

Computer simulations based on experimental data indicate that long wavelength pigments in PS I are likely to be located in the vicinity of the trap (Jia et al., 1992). It is not clear if the trapping is limited by slow energy transfer from the long wavelength pigments to P700 (due to either energetic constraints or the distance between the donor and acceptor or both) or by the charge separation. Strictly speaking, the former scenario is defined as diffusion limited; however, it depends on a precise definition of what is considered to be the trap. This special case has been termed the pseudo-trap-limited or special-trap-limited case (van Grondelle & Sundström, 1988; Otte et al., 1993). It has recently been suggested that this special-trap-limited case may be appropriate for purple bacterial membrane fragments (Otte et al., 1993).

The pseudo-trap-limited model postulates that the excited singlet state of P700 (P700*) is not included in the thermally relaxed distribution that occurs prior to trapping. In the analysis of Holzwarth et al. (1993) it is assumed that P700* is in equilibrium with the spectrally equilibrated antenna pigments. They do not consider a special-trap-limited model, although their data appear to be equally consistent with such a model. The fluorescence and transient absorption data presented here [and by Holzwarth et al. (1993)] are not sufficient to unambiguously distinguish between the two trapping-limited cases.

We show in the following paper that the intrinsic rate of radical pair formation in the PS I particles used here must be less than $(4\ ps)^{-1}$. It is also possible to estimate an upper limit for the intrinsic rate of radical pair formation from the data presented here, by using an approach similar to that outlined by Trissl et al. (1993) [see also Trissl (1993) and Lin et al. (1994)], in which it is assumed that the kinetics in the PS I core antenna can be described by a purely trapping-limited model. The PS I core antenna is spectrally heterogeneous, and since trapping occurs from a spectrally equilibrated distribution of pigments, the actual number of antenna pigments coupled to the charge separation process is reduced. To calculate the intrinsic rate of radical pair formation, it is necessary to calculate the effective number of pigments that are isoenergetic with the longest wavelength absorbing pigments (Trissl, 1993). Calculation of this effective antenna size requires knowledge of the spectral composition of the core antenna. We show above that there are about 98 Chl *a*/P700. Assuming that there are ~8 chlorophylls that absorb at 703 nm (Woolf et al., 1994) with the remaining 90 chlorophylls absorbing at 680 nm, an effective antenna size of 17 is calculated. Using this effective antenna size and a Stokes shift of 6 nm for Chl *a*, 12 nm for P700 (Trissl, 1993), and the observed 28-ps trapping time, we calculate that the intrinsic time constant characterizing radical pair formation in the PS I particles used here is 1.6 ps.

Using the pigment stoichiometries calculated by Holzwarth et al. (1993) for their PS I particles from *Synechococcus* sp. and their overall excitation decay time of 35 ps, we estimate that the intrinsic time constant characterizing radical pair formation in that species is 1.5 ps. In a similar calculation, using an observed trapping time of 80 ps, Trissl et al. (1993) calculated a 2.3-ps intrinsic time constant for radical pair formation in PS I stacked pea thylakoids.

The calculations outlined above implicitly assume that the trapping process is described by a purely trapping-limited model, in which time constants for energy transfer between neighboring antenna pigments (one of which is the primary electron donor) are much smaller than the time constant for charge separation. It can be shown that [assuming a model in which the antenna system is described by a regular array of equidistant pigments (Pearlstein, 1982)], if the time constants governing any of the energy transfer processes increase or become rate-limiting (which results in an increase in the first passage time), the intrinsic time constant governing radical pair formation can only decrease for the same observed trapping time (Pearlstein, 1982; Lin et al., 1994). Therefore, the calculated time constant of 1.6 ps represents an upper limit for the ($P700^* \rightarrow P700^+A_0^-$) process.

CONCLUSIONS

The results and interpretation of the fluorescence and transient absorption data are in excellent agreement. In the past it has been difficult to reconcile fluorescence and absorption measurements (Holzwarth et al., 1991). Such good agreement between both fluorescence and absorption techniques may be due to the fact that we have used low levels of excitation in our transient absorption measurements, eliminating complicating effects due to exciton annihilation.

Both fluorescence and transient absorption measurements indicate that the excitation energy equilibrates among all the different spectral forms in the core antenna in 4–6 ps. The spectra associated with the equilibration process indicate the presence of long wavelength pigments in the core antenna. Trapping occurs from this equilibrated distribution of antenna chlorins with a time constant of 24–28 ps. Trapping results in a difference spectrum that is due only to $P700^+$ formation. The intrinsic rate of radical pair formation in the PS I particles used here is 1.6 ps or less, but the details of the kinetic processes that underlie the trapping of excitations remain unclear at present.

The kinetics appear to be similar in another cyanobacterial PS I particle. However, the organization and/or composition of the core antenna appears to be somewhat different.

ACKNOWLEDGMENT

We thank Wim Vermaas and Cathy Madsen for providing cells of the PS II deletion mutant of *Synechocystis* sp. PCC 6803 and advice on growth procedures. This is publication 181 from the Arizona State University Center for the Study of Early Events in Photosynthesis.

REFERENCES

Beauregard, M., Martin, I., & Holzwarth, A. R. (1991) *Biochim. Biophys. Acta 1060*, 271–283.

Boekema E. J., Dekker, J. P., van Heel, M. G., Rogner, M., Saenger, W., Witt, I., & Witt, H. T. (1987) *FEBS Lett. 217*, 283–286.

Butler, W. L. (1978) *Annu. Rev. Plant Physiol. 29*, 345–378.

Cantrell, A., & Bryant, D. A. (1987) *Plant Mol. Biol. 9*, 453–468.

Causgrove, T. P., Yang, S., & Struve, W. S. (1988) *J. Phys. Chem. 92*, 6121–6124.

Causgrove, T. P., Brune, D. C., Olsen, J. M., & Blankenship, R. E. (1990) *Photosynth. Res. 25*, 1–10.

Du, M., Xie, X., Jia, Y., Mets, L., & Fleming, G. R. (1992) *Chem. Phys. Lett. 201*, 535–542.

Fischer, M. J., & Hoff, A. J. (1992) *Biophys. J. 63*, 911–916.

Hefti, A., Ford, R. C., Miller, M., Cox, R. P., & Engel, A. (1992) *FEBS Lett. 296*, 29–32.

Hiyama, T., & Ke, B. (1972) *Biochim. Biophys. Acta 267*, 160–171.

Hodges, M., & Moya, I. (1988) *Biochim. Biophys. Acta 935*, 41–52.

Hoff, A. J., & Amesz, J. (1991) in *The Chlorophylls* (Scheer, H., Ed.) pp 723–738, CRC Press, Boca Raton, FL.

Holzwarth, A. R. (1989) *Q. Rev. Biophys. 22*, 269–295.

Holzwarth, A. R. (1991) in *The Chlorophylls* (Scheer, H., Ed.) pp 1126–1151, CRC Press, Boca Raton, FL.

Holzwarth, A. R., Schatz, G. H., Brock, H., & Bittersman E. (1993) *Biophys. J. 64*, 1813–1826.

Ikegami, I., & Itoh, S. (1988) *Biochim. Biophys. Acta 934*, 39–46.

Jia, Y., Jean, J. M., Werst, M. M., Chan, C., & Fleming, G. R. (1992) *Biophys. J. 63*, 259–273.

Klug, D. R., Gore, B. L., Giorgi, L. B., & Porter, G. (1987) in *Progress in Photosynthesis Research* (Biggins, J., Ed.) Vol. I, pp 95–98, Nijhoff, Dordrecht, The Netherlands.

Klug, D. R., Giorgi, L. B., Crystal, B., Barber, J., & Porter, G. (1989) *Photosynth. Res. 22*, 277–284.

Laible, P. D., & Owens, T. G. (1993) *Photochem. Photobiol. 57S*, 17S.

Lin, S., Chiou, H.-C., Kleinherenbrink, F. A. M., & Blankenship, R. E. (1994) *Biophys. J. 66*, 437–445.

Martin, J.-L., & Vos, M. H. (1992) *Annu. Rev. Biophys. Biomol. Struct. 21*, 199–222.

Nechushtai, R., Nourizadeh, S. D., & Thornber, J. P. (1986) *Biochim. Biophys. Acta 1143*, 84–90.

Otte, S. C. M., Kleinherenbrink, F. A. M., & Amesz, J. (1993) *Biochim. Biophys. Acta 848*, 193–200.

Owens, T. G., Webb, S. P., Mets, L., Alberte, R. S., & Fleming, G. R. (1987) *Proc. Natl. Acad. Sci. U.S.A. 84*, 1532–1536.

Owens, T. G., Webb, S. P., Alberte, R. S. Mets, L., & Fleming, G. R. (1988) *Biophys. J. 53*, 733–745.

Pearlstein, R. M. (1982) *Photosynthesis: Energy Conversion by Plants and Bacteria* (Govindjee, Ed.) Vol. 1, pp 294–330, Academic Press, New York.

Satoh, K., & Butler, W. L. (1978) *Biochim. Biophys. Acta 502*, 103–110.

Schaffernicht, H., & Junge, W. (1981) *Photochem. Photobiol. 34*, 223–232.

Schaffernicht, H., & Junge, W. (1982) *Photochem. Photobiol. 36*, 111–115.

Schatz, G. H., Brock, H., & Holzwarth, A. R. (1987) *Proc. Natl. Acad. Sci. U.S.A. 84*, 8414–8418.

Sétif, P. (1992) Topics in Photosynthesis 11, in *The Photosystems: Structure, Function and Molecular Biology* (Barber, J., Ed.) pp 471–499, Elsevier Science Publishers, New York.

Struve, W. (1990) *J. Opt. Soc. Am. B7*, 1586–1593.

Taguchi, A. K. W., Stocker, J. W., Alden, R. G., Causgrove T. P., Peloquin, J. M., Boxer, S. G., & Woodbury, N. W. (1992) *Biochemistry 31*, 10345–10355.

Trissl, H.-W. (1993) *Photosynth. Res. 35*, 247–263.

Trissl, H.-W., Hecks, B., & Wulf, K. (1993) *Photochem. Photobiol. 57*, 108–112.

Turconi, S., Schweitzer, G., & Holzwarth, A. R. (1993) *Photochem. Photobiol. 57*, 113–119.

van Grondelle, R. (1985) *Biochim. Biophys. Acta 811*, 147–195.

van Grondelle, R., & Sundström, V. (1988) in *Photosynthetic Light Harvesting Systems* (Scheer, H., & Schneider, S., Eds.) pp 403–438, Gruyter, Berlin.

Vermaas, W. F. J., Williams, J. G. K., & Arntzen, C. J. (1987) *Z. Naturforsch 42c*, 762–768.

Vermaas, W. F. J., Ikeuchi, M., & Inoue, Y. (1988) *Photosynth. Res. 17*, 97–113.

Werst, M. M., Jia, Y., Mets, L., & Fleming, G. R. (1992) *Biophys. J. 61*, 868–878.

Wittmershaus, B. P., Berns, D. S., & Huang, C. (1987) *Biophys. J. 52*, 829–836.

Wittmershaus, B. P., Woolf, V. M., & Vermaas, W. F. J. (1992) *Photosynth. Res. 31*, 75–87.

Woolf, V. M., Wittmershaus, B. P., Vermaas, W. F. J., & Tran, T. D. (1994) *Photosynth. Res.* (in press).